

Photocatalytic properties of amorphous and graphitic carbon dots based on citric acid

© I.V. Margaryan¹, A.M. Mitroshin^{1,2}, N.B. Viktorov³, A.Yu. Dubavik¹, S.A. Kurnosenko⁴,
O.I. Silyukov⁴, E.V. Kundelev^{1,*}

¹ International research and educational center for physics of nanostructures, ITMO University, Saint-Petersburg, Russia

² Institute of Macromolecular Compounds, Russian Academy of Sciences, St. Petersburg, Russia

³ St. Petersburg State Technological Institute (Technical University), St. Petersburg, Russia

⁴ St. Petersburg State University, St. Petersburg, Russia

*e-mail: kundelev.evg@gmail.com

Received April 24, 2024

Revised April 24, 2024

Accepted April 27, 2024

The simplicity of synthesis of carbon dots with the required energetic and optical properties determines the interest in their use as photoabsorbers in photocatalytic hydrogen generation systems. In order to effectively use carbon dots with the desired characteristics, proper purification of carbon dots from low molecular weight reaction products, which can significantly alter the final properties of carbon dots, is critical. In this work, amorphous and graphitic carbon dots were prepared from citric acid and their purification procedure was carried out. Further, structural, optical and photocatalytic characterization of both the initial and purified carbon dots was performed. Analysis of the obtained data showed that low molecular weight reaction products contribute significantly to the ability of photocatalytic systems to generate hydrogen. The application of a proper procedure for purification of carbon dots is essential to obtain correct results in photocatalytic hydrogen generation experiments.

Keywords: photocatalysis, hydrogen generation, carbon dots, photoluminescence, luminescence decay time, atomic force microscopy, infrared absorption spectroscopy.

DOI: 10.61011/EOS.2024.05.59121.6387-24

Introduction

Carbon dots (CD) are classified as carbon-based nanomaterials whose internal structure [1–5] includes a carbonized core and numerous molecular-type optical centers [4,6–11]. Such CD structure with numerous various optical centers accounts for dependence of PL on excitation wavelength. The presence of bright, stable and tunable PL of CD in a wide visible spectrum range determines extensive application of CDs in sensorics and optoelectronic devices [12–15]. Easy synthesis of CDs capable of absorbing solar radiation from ultraviolet to infrared spectrum range allows them to be used as absorbers in photocatalytic systems [16,17]. At this point, various CDs have been used in photocatalytic hydrogen generation systems mainly without a proper procedure for removing low-molecular synthesis-by-products (dialysis) [16,17]. The lack of CD dialysis procedure may lead to incorrect results of photocatalytic hydrogen generation experiments.

In this study, structural and optical properties of amorphous and graphitic CDs based on citric acid have been identified and also investigated at various synthesis temperatures. Atomic force spectroscopy, IR absorption spectroscopy, UV-VIS absorption and luminescence spectroscopy have been used to identify and investigate structural and optical properties of amorphous and graphitic CDs before and after the dialysis procedure. The obtained CDs used as light absorbers together with the Du Bois

type $[\text{Ni}(\text{P}_2\text{N}_2)_2]^{2+}$ catalyst containing an external coordination sphere with phosphonic groups has made it possible to identify the influence of low-molecular organic matter formed as by-product during the CD synthesis process on the hydrogen generated capabilities of a composite photocatalytic system. Analysis of the obtained data has shown that a proper CD purification procedure was necessary to obtain correct results of the photocatalytic hydrogen generation experiments.

1. Materials and research methods

Amorphous CDs (*a-CDots*) were synthesized using a technique described in [16]. For this, 2 g of citric acid (*CA*) was heated in an open crucible in a muffle furnace at 180°C for 40 h to form of a viscous dark brown liquid. 2.3 mL of water and aqueous NaOH solution (5M, 1.35 mL) were added to the prepared solution for neutralization to pH 7. Then, the freeze-drying method was used to isolate CDs *CDots* in the form of 0.9 g yellow-orange powder coated with sodium carboxylates. Synthesis of these CDs was not followed by a dialysis procedure. To obtain amorphous CDs free from low-molecular reaction products (*a-CDots-D*), a *a-CDots* dialysis procedure was employed with the use of a 3.5 kDa membrane during 7 days.

Graphitic CDs (*g-CDots*) were synthesized similar to the synthesis of amorphous CDs (*a-CDots*) using additional

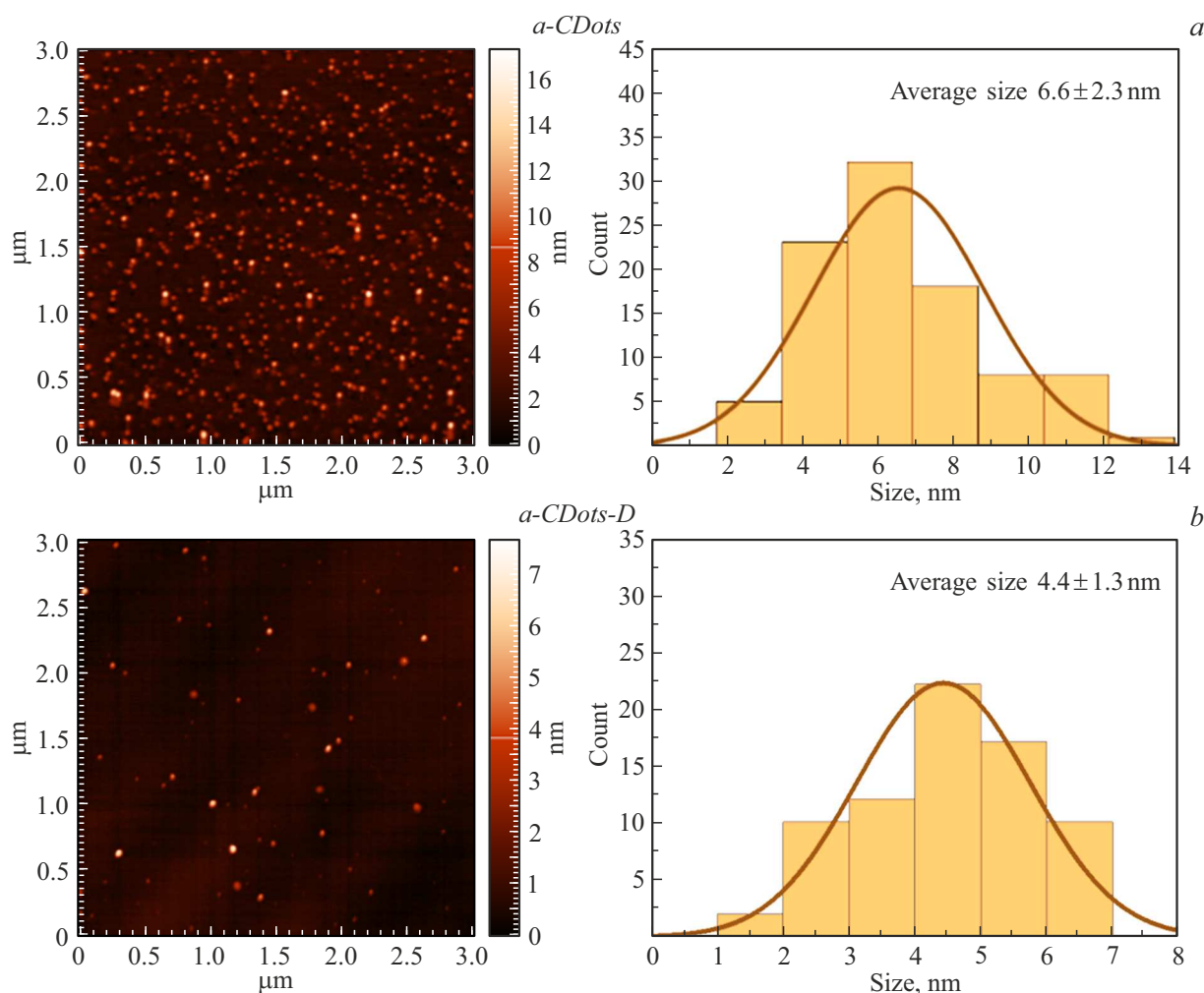


Figure 1. AFM images for CDs *a-CDots* and *a-CDots-D* and corresponding size distribution histograms.

high-temperature treatment [17]. For this, at the first stage 2 g of citric acid underwent pyrolysis in an open crucible in a muffle furnace at 180°C during 40 h. Then, additional heating at 320°C during 100 h was used. The obtained product was dissolved in 3 mL of water and neutralized to pH 7 by adding aqueous NaOH solution (5 M, 0.45 mL) to obtain CDs coated with sodium carboxylates. Then, freeze-drying method was used to isolate *g-CDots* in the form of yellow-orange powder. *g-CDots-D* free from low-molecular reaction products were obtained similar to the procedure used for amorphous CDs.

Synthesis of the Du Bois type (NiP) water soluble catalyst containing the electroactive $[\text{Ni}(\text{P}_2\text{N}_2)_2]^{2+}$ core with an external coordination sphere in the form of four phosphonic acid fragments was conducted using a technique described in [18].

The absorption spectra of CDs were recorded using the UV-3600 spectrophotometer (Shimadzu, Japan). CD luminescence and luminescence excitation spectra were measured using the Cary Eclipse spectrofluorimeter (Varian, Australia). FTIR absorption spectra of CDs were recorded

using the Tensor II IR spectrophotometer (Bruker, USA) in the attenuated total internal reflection mode.

The size of CDs was obtained using the Solver Pro-M atomic force microscope (AFM) (NT-MDT, Russia). For this, $70 \mu\text{L}$ of CD solution was applied to the mica surface by centrifugation with the following parameters: 5 s at 500 r/min and 25 s at 2000 r/min. After subsequent annealing of CDs during 15 min at 130° , CD sizes were measured.

The MicroTime100 scanning laser microscope (PicoQuant, Germany) was used to record CD PL decay curves approximated by the biexponential function

$$I = A_1 e^{-\frac{t}{\tau_1}} + A_2 e^{-\frac{t}{\tau_2}}. \quad (1)$$

The mean CD PL decay time was calculated using the following equation

$$\tau_{av} = \frac{\sum_i A_i \tau_i^2}{\sum_i A_i \tau_i}, \quad (2)$$

where A_i and τ_i are the amplitude and decay time of the i component, respectively.

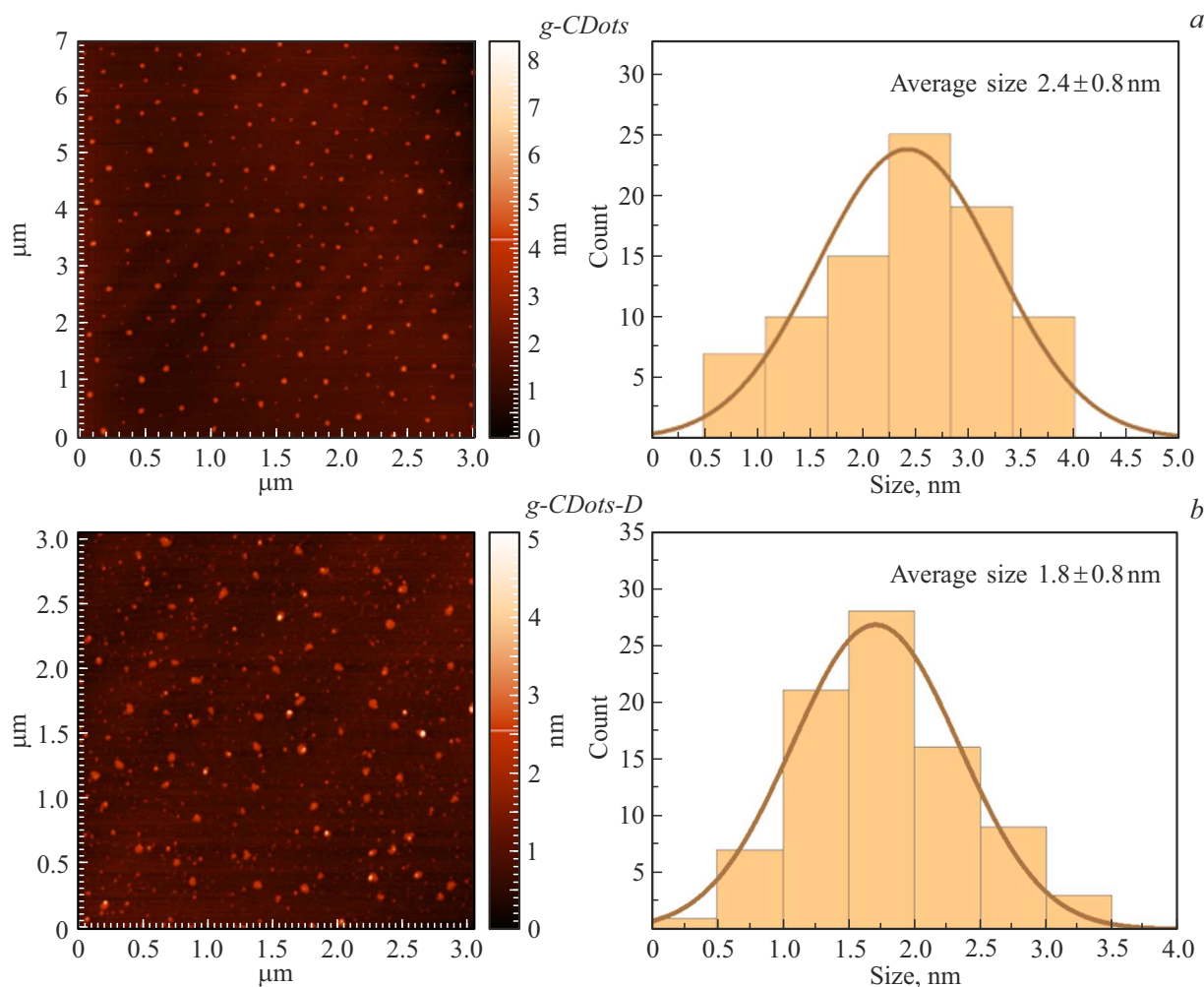


Figure 2. AFM images for CDs *g-CDots* and *g-CDots-D* and corresponding size distribution histograms.

For the purpose of photocatalytic experiments, 167 mg (10 nmol) of CDs and 0.27 mg (10 nmol) of NiP catalyst were mixed in 50 mL of 0.1 M ethylenediaminetetraacetic acid (EDTA, electron donor) aqueous solution with pH 6 and shaken in a vortex mixer during 1 min. Then, the mixture was placed into a reaction cell and thermostating was initiated (20°C). For photoexcitation of the photocatalytic system, the Osram XBO-150 lamp and light filtering NaBr and KCl mixture solution were used to obtain exciting light from 220 nm. Then, the system was purged with argon during 30 min, gas chromatographic analysis was started for the total time of 4 h with sampling every 15 min.

Results and discussion

Figure 1 shows AFM images for amorphous *a-CDots* (a) and *a-CDots-D* (b) with corresponding size distribution histograms. For *a-CDots* obtained without dialysis procedure, a mean size of $6.6 \pm 2.3 \text{ nm}$ is typical, which agrees with the sizes previously determined by the high-resolution transmission electron microscopy (TEM) for

similarly obtained CDs [16]. The size distribution histogram of dialyzed *a-CDots-D* in Figure 2, b shows that their mean size decreases to $4.4 \pm 1.3 \text{ nm}$. Decrease in the mean sizes of CDs after removal of low-molecular synthesis products may be indicative of weak coupling of CD components or centers. According to the AFM images and corresponding size distribution histograms shown in Figure 2, mean sizes $2.4 \pm 0.8 \text{ nm}$ and $1.8 \pm 0.8 \text{ nm}$ are typical for ordinary *g-CDots* and dialyzed *g-g-CDots-D*. Note that the dialysis of graphitic as well as amorphous CDs leads to the decrease in their mean size.

The surface structure of original amorphous and graphitic *a-CDots* and *g-CDots*, and of purified equivalent *a-CDots-D* and *g-CDots-D* was identified using the IR absorption spectroscopy. Figure 3 shows IR absorption spectra of *a-CDots*, *a-CDots-D* and NaOH-neutralized citric acid (CA) precursor for comparison. The FTIR spectra of amorphous *a-CDots* and *a-CDots-D* are characterized by two characteristic bands at 1396 and 1566 cm^{-1} , corresponding to symmetric and asymmetric stretching of sodium carboxylates on the CD surface. The similar stretching

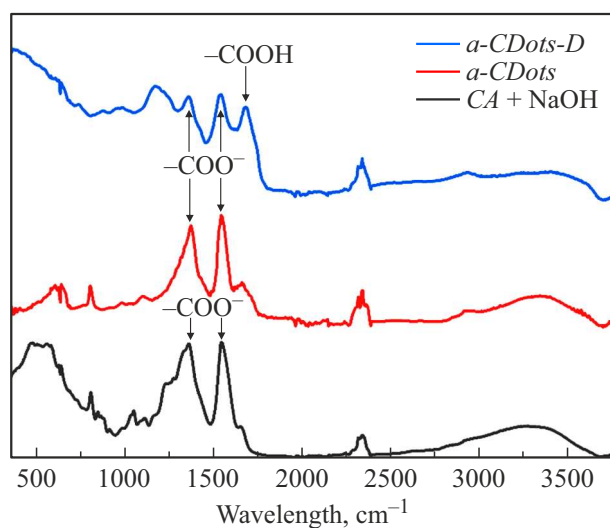


Figure 3. FTIR absorption spectra of *a-CDots*, *a-CDots-D* and NaOH-neutralized CA molecules. Characteristic frequencies are marked with arrows.

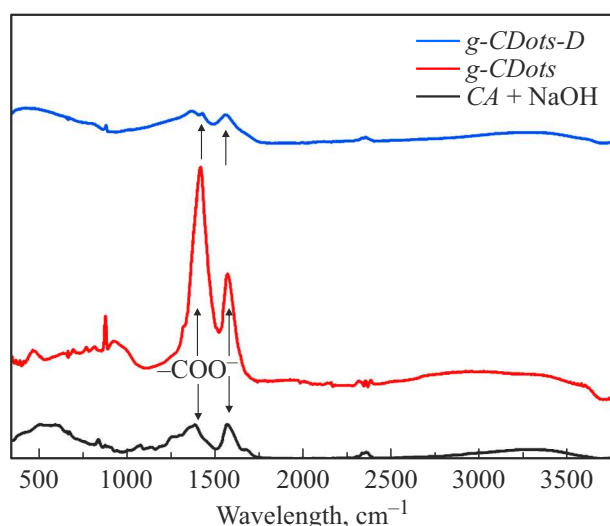


Figure 4. FTIR absorption spectra of *g-CDots*, *g-CDots-D* and NaOH-neutralized CA molecules. Characteristic frequencies are marked with arrows.

bands of the sodium carboxylates of the molecular CA precursor are located at 1385 and 1566 cm^{-1} . The IR absorption spectrum of amorphous dialyzed *a-CDots-D* is also characterized by a carboxyl group ($-\text{COOH}$) stretching band at 1703 cm^{-1} . Graphitic CDs have characteristic IR absorption bands (Figure 4) at 1417 and 1570 cm^{-1} (*g-CDots*) and 1427 and 1564 cm^{-1} (*g-CDots-D*) that are also referred to sodium carboxylate stretching on the CD surface.

Figure 5 shows absorption and luminescence spectra of amorphous and graphitic CDs. The absorption spectra of amorphous *a-CDots* and *a-CDots-D* are characterized by absorption up to 500 and 600 nm with a typical arm

in the area of 250 nm . Graphitic *g-CDots* and *g-CDots-D* have absorption up to the near IR spectrum range (700 nm) with even more pronounced arm at $250\text{--}300\text{ nm}$. The absorption spectra structure of both amorphous and graphitic CDs is in full agreement with that for previously obtained CDs [16,17,19]. When recorded at 460 nm and 450 nm , the luminescence excitation spectra of the amorphous and graphitic CDs have a structure with two peaks in the area of $250\text{--}350\text{ nm}$. For amorphous CDs, higher intensity of the long-wavelength peak is observed, while for graphitic CDs, the short-wavelength peak is more intense. Note that disagreement of the type absorption spectra with the corresponding luminescence excitation spectra of both amorphous and graphitic CDs is indicative of a contribution of a large number of absorption centers of CD to the observed amorphous spectrum of CDs. From Figure 5, *a*, it is clear that the PL peak position and intensity for amorphous *a-CDots* and *a-CDots-D* depend on the excitation wavelength; when the excitation wavelength shifts from $\lambda = 360$ to 460 nm , the emission maximum shifts from $\lambda = 459$ for *a-CDots* and from $\lambda = 470$ to 554 nm for *a-CDots-D*, and a significant drop in the PL intensity occurs [3]. A similar dependence of the PL peak is observed for graphitic *g-CDots* and *g-CDots-D* (Figure 6, *a, b*). Excitation wavelength shift for graphitic *g-CDots* from $\lambda = 300$ to 420 nm leads to the shift of their PL peak from $\lambda = 440$ to 524 nm . The dialyzed amorphous and graphitic carbon dots CD are also characterized by wider luminescence bands. The most intense PL band of dialyzed amorphous *a-CDots-D* with excitation at 360 nm has a full width at half maximum that is 27 nm larger than that for the similar PL band of the original *a-CDots* (102 nm). For graphitic CDs, the difference in the width of more intense luminescence peaks between dialyzed *g-CDots-D* and original *g-CDots* achieves 103 nm . The observed features in the PL spectra of dialyzed *a-CDots-D* and *g-CDots-D* in the form of wider PL peaks and more intense long-wavelength PL may indicate that the CD dialysis process leads to a slight change in the structure of a part of the optical centers on the CD surface, which is also proved by the change in luminescence excitation spectra of the original and dialyzed CDs.

Figure 7,8 shows the PL decay kinetics of amorphous and graphitic CDs with excitation at 410 nm . When approximating the PL decay curves by biexponential function (1), mean decay times of 4.0 and 3.3 ns were obtained for the original and dialyzed amorphous (*a-CDots* and *a-CDots-D*), as well as 2.6 and 4.2 ns were obtained or original and dialyzed graphitic (*g-CDots* and *g-CDots-D*), that were calculated according to expression (2). The data obtained are consistent with the typical PL decay times for CDs [16,17,19]. Variation of the decay times for original and dialyzed amorphous and graphitic CDs may indicate that the dialysis of carbon dots leads not only to some change in the structure of a part of optical centers on the surface, but also affects the relation between radiative and nonradiative relaxation rates of photoexcitations in CDs.

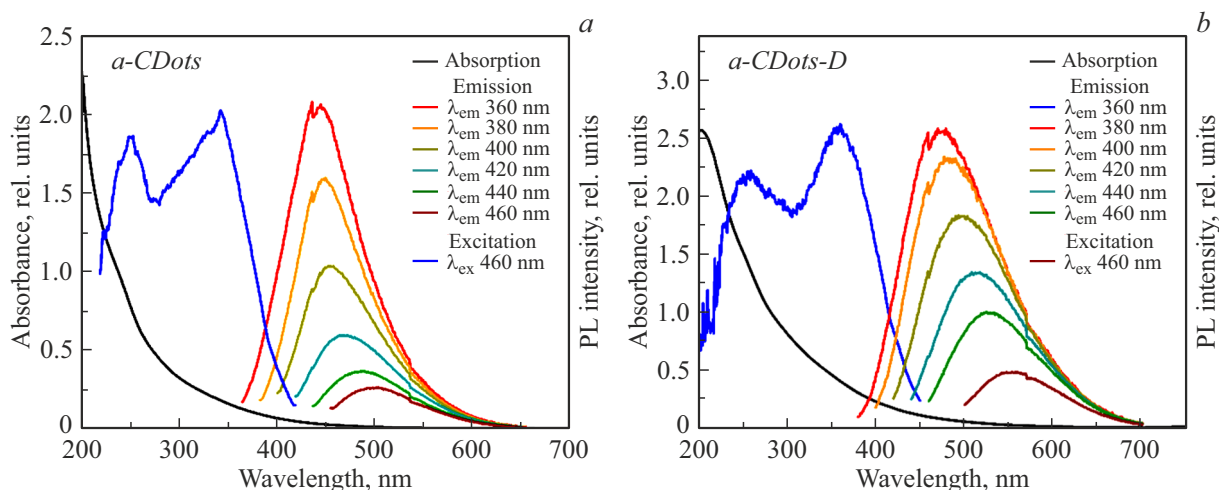


Figure 5. Absorption, PL and PL excitation spectra of *a-CDots* (a) and *CDots-D* (b) at different excitation and recording wavelengths, as shown in the figure legend.

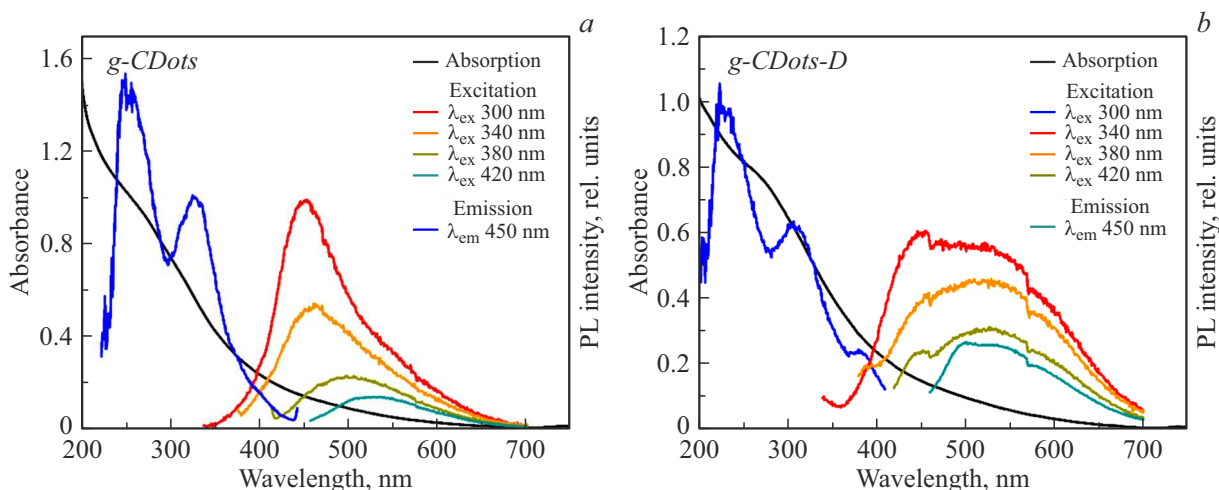


Figure 6. Absorption, PL and PL excitation spectra of *g-CDots* (a) and *g-CDots-D* (b) at different excitation and recording wavelengths, as shown in the figure legend.

The photocatalytic hydrogen generation experiments by the CD/NiP system (with molar ratio 1:1) were conducted in water with pH 6 with addition of the electron donor in the form of EDTA. Figure 9 shows the outlines of hydrogen generation for various photoabsorbers in the form of CDs: original amorphous (*a-CDots*) and dialyzed (*a-CDots-D*) as well as original graphitic (*g-CDots*) and dialyzed (*g-CDots-D*). When using amorphous *a-CDots* in photocatalysis, 30.3 μL of hydrogen is generated during 4 h, while in case of similar dialyzed (*a-CDots-D*), only 8.8 μL of hydrogen is generated during the same time. More than a three-fold decrease in hydrogen generation for dialyzed CDs compared with the original equivalent CDs is indicative of a significant contribution of low-molecular organic matter to hydrogen generation. For graphitic CDs, generation of 13.6 μL and 16.8 μL for original *g-CDots* and dialyzed *g-CDots-D* is observed. Although low-molecular organic

matter does not make any considerable contribution to the total volume of hydrogen generation, the presence of low-molecular organic matter has significant influence on the hydrogen generation rate (turnover frequency, TOF) during the experiment. Thus, for original graphitic (*g-CDots*) TOF (1 h) for the first hour is 37, while for dialyzed CDs (*g-CDots-D*) it is only 12. After 2 h of the photocatalytic experiment, hydrogen generation when using *g-CDots* almost stops, while for dialyzed CDs *g-CDots-D*, the hydrogen generation rate even increases with time. Various features observed when CD are used in photocatalysis before and after dialysis are indicative of the considerable contribution of low-molecular organic matter to the resultant hydrogen generation figures. Thus, for photocatalytic hydrogen generation experiments, it is critical to remove properly low-molecular organic matter and unify this process to provide the results applicable to

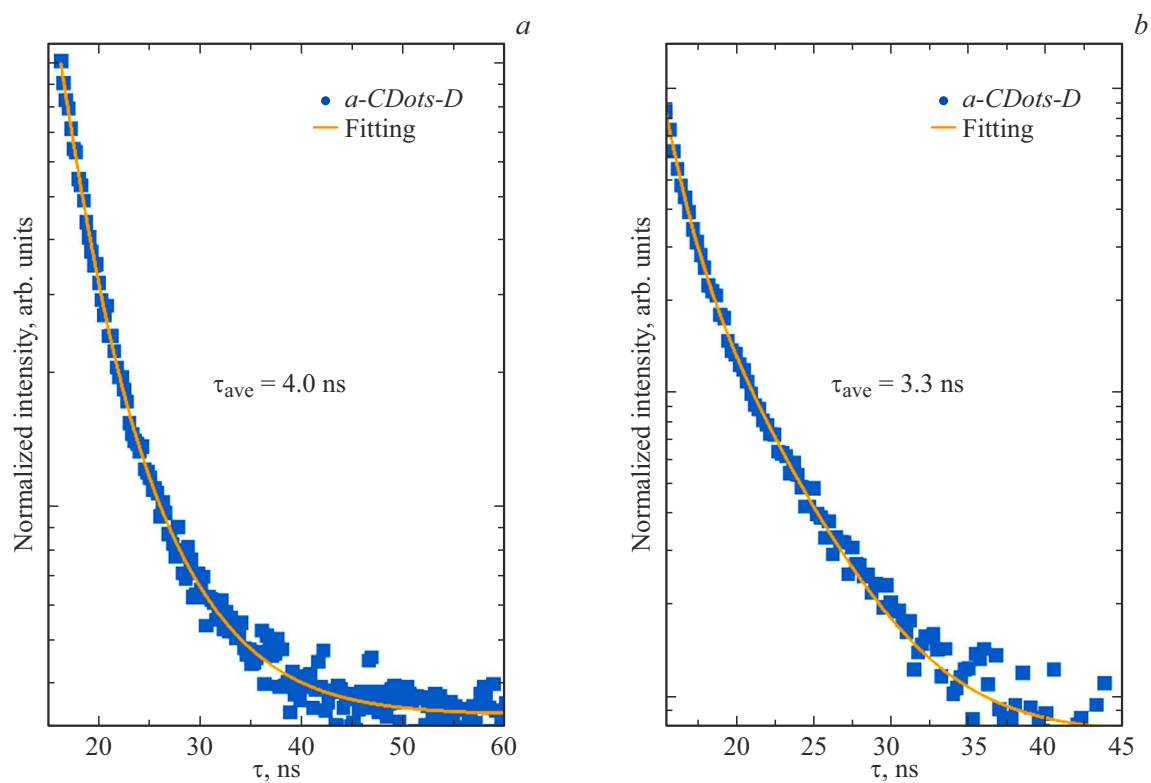


Figure 7. PL decay curves of *a-CDots* (a) and *a-CDots-D* (b) with excitation at 410 nm.

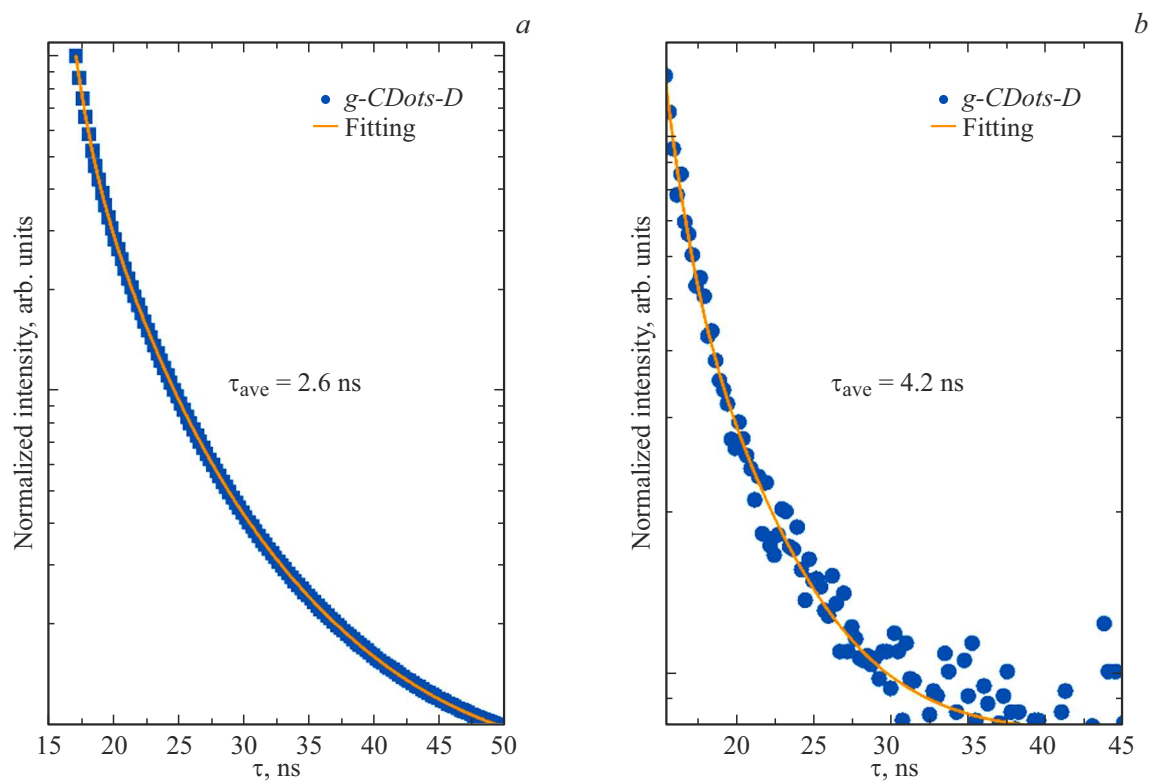


Figure 8. PL decay curves of *g-CDots* (a) and *g-CDots-D* (b) with excitation at 410 nm.

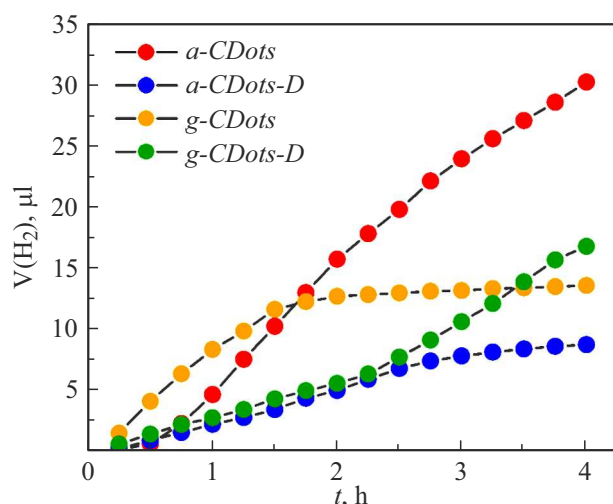


Figure 9. Outlines of hydrogen generation by photocatalytic CD/NiP systems (CD: *a-CDots*, *a-CDots-D*, *g-CDots*, *g-CDots-D*) in water at pH 6 using EDTA as the electron donor.

CDs and correct comparison with other photoabsorbers in photocatalytic hydrogen generation systems.

Conclusion

This study has obtained and investigated the structural and optical properties of amorphous and graphitic CDs based on citric acid at the synthesis temperatures from 180 to 320°C. The atomic force spectroscopy has been used to measure the sizes of amorphous and graphitic CDs before and after dialysis (6.6 ± 2.3 , 4.4 ± 1.3 , 2.4 ± 0.8 and 1.8 ± 0.8 nm for *a-CDots*, *a-CDots-D*, *g-CDots*, *g-CDots-D*). Analysis of IR absorption spectra has shown that the surface of both amorphous and graphitic CDs is characterized by the presence of carboxyl groups. The optical properties of CDs have been investigated using UV-VIS absorption spectroscopy and luminescence spectroscopy. It has been found that amorphous and graphitic CDs have molecular optic centers that define main photophysical properties of CDs in the visible spectrum range. The obtained CDs used as light absorbers in a composite water photocatalytic system together with the Du Bois type $[\text{Ni}(\text{P}_2\text{N}_2)_2]^{2+}$ molecular catalyst containing an external coordination sphere with phosphonic groups has made it possible to identify the influence of the type of CD and of the CD dialysis procedures on the hydrogen generation. It has been first shown that low-molecular organic matter formed as by-product during CD synthesis has a significant influence on the hydrogen generating capabilities of the composite photocatalytic system. Thus, provision of a proper CD purification procedure is necessary to obtain correct results of the photocatalytic hydrogen generation experiments.

Funding

The study was funded by the Russian Science Foundation as part of research project № 22-73-00141.

Conflict of interest

The authors declare that they have no conflict of interest.

References

- [1] X. Xu, R. Ray, Y. Gu, H. J. Ploehn, L. Gearheart, K. Raker, W. A. Scrivens. *J. Am. Chem. Soc.*, **126** (40), 12736–12737 (2004). DOI: 10.1021/ja040082h
- [2] S.N. Baker, G.A. Baker. *Angew. Chem. Int. Ed. Engl.*, **49** (38), 6726–6744 (2010). DOI: 10.1002/anie.200906623
- [3] L. Xiao, H. Sun. *Nanoscale Horiz.*, **3** (6), 565–597 (2018). DOI: 10.1039/c8nh00106e
- [4] S. Zhu, Q. Meng, L. Wang, J. Zhang, Y. Song, H. Jin, K. Zhang, H. Sun, H. Wang, B. Yang. *Angew. Chem. Int. Ed. Engl.*, **52** (14), 3953–3957 (2013). DOI: 10.1002/anie.201300519
- [5] F. Yuan, Z. Wang, X. Li, Y. Li, Z. Tan, L. Fan, S. Yang. *Adv. Mater.*, **29** (3), 1604436 (2017). DOI: 10.1002/adma.201604436
- [6] N.V. Teplakov, E.V. Kundelev, P.D. Khavlyuk, Y. Xiong, M.Y. Leonov, W. Zhu, A.V. Baranov, A.V. Fedorov, A.L. Rogach, I.D. Rukhlenko. *ACS Nano*, **13** (9), 10737–10744 (2019). DOI: 10.1021/acsnano.9b05444
- [7] Y.F. Kang, Y.H. Li, Y.W. Fang, Y. Xu, X.M. Wei, X.B. Yin. *Sci. Rep.*, **5**, 11835 (2015). DOI: 10.1038/srep11835
- [8] E.A. Stepanidenko, I.A. Arefina, P.D. Khavlyuk, A. Dubavik, K.V. Bogdanov, D.P. Bondarenko, S.A. Cherevko, E.V. Kundelev, A.V. Fedorov, A.V. Baranov, V.G. Maslov, E.V. Ushakova, A.L. Rogach. *Nanoscale*, **12** (2), 602–609 (2020). DOI: 10.1039/c9nr08663c
- [9] E.V. Kundelev, N.V. Teplakov, M.Y. Leonov, V.G. Maslov, A.V. Baranov, A.V. Fedorov, I.D. Rukhlenko, A.L. Rogach. *J. Phys. Chem. Lett.*, **11** (19), 8121–8127 (2020). DOI: 10.1021/acs.jpcclett.0c02373
- [10] E.V. Kundelev, N.V. Teplakov, M.Y. Leonov, V.G. Maslov, A.V. Baranov, A.V. Fedorov, I.D. Rukhlenko, A.L. Rogach. *J. Phys. Chem. Lett.*, **10** (17), 5111–5116 (2019). DOI: 10.1021/acs.jpcclett.9b01724
- [11] E.V. Kundelev, E.D. Strievich, N.V. Teplakov, A.D. Murkina, A.Y. Dubavik, E.V. Ushakova, A.V. Baranov, A.V. Fedorov, I.D. Rukhlenko, A.L. Rogach. *J. Phys. Chem. C*, **126** (42), 18170–18176 (2022). DOI: 10.1021/acs.jpcc.2c05926
- [12] X. Shan, L. Chai, J. Ma, Z. Qian, J. Chen, H. Feng. *Analyst*, **139** (10), 2322–2325 (2014). DOI: 10.1039/c3an02222f
- [13] A.H. Loo, Z. Sofer, D. Bouša, P. Ulbrich, A. Bonanni, M. Pumera. *ACS Appl. Mater. Interfaces*, **8** (3), 1951–1957 (2016). DOI: 10.1021/acsami.5b10160
- [14] H. Yu, Y. Zhao, C. Zhou, L. Shang, Y. Peng, Y. Cao, L.Z. Wu, C.H. Tung, T. Zhang. *J. Mater. Chem. A*, **2**, 3344–3351 (2014). DOI: 10.1002/cssc.201700943
- [15] X. Zhang, Y. Zhang, Y. Wang, S. Kalytchuk, S.V. Kershaw, Y. Wang, P. Wang, T. Zhang, Y. Zhao, H. Zhang. *ACS Nano*, **7** (12), 11234–11241 (2013). DOI: 10.1021/nn405017q
- [16] B.C.M. Martindale, G.A.M. Hutton, C.A. Caputo, E. Reisner. *J. Am. Chem. Soc.*, **137** (18), 6018–6025 (2015). DOI: 10.1021/jacs.5b01650

- [17] B.C.M. Martindale, G.A.M. Hutton, C.A. Caputo, S. Prantl, R. Godin, J.R. Durrant, E. Reisner. *Angew. Chem. Int. Ed. Engl.*, **129** (23), 6559–6463 (2017). DOI: 10.1002/anie.201700949
- [18] M.A. Gross, A. Reynal, J.R. Durrant, E. Reisner. *J. Am. Chem. Soc.*, **136** (1), 356–366. (2014). DOI: 10.1021/ja410592d
- [19] I.V. Margaryan, A.M. Mitroshin, A.Yu. Dubovik, E.V. Kundelev. *Opt. i spectr.*, **131** (7), 985 (2023). (in Russian) DOI: 10.61011/EOS.2024.05.59121.6387-24

Translated by E.Ilinskaya